

Seasonal Assessment of Fluoride Contamination in Drinking Water Aquifers of Kota District, Rajasthan

Priyanshi Sharma¹, Dr. Shikha Verma²

¹Department of Life Sciences, Pacific Academy of Higher Education and Research University, Udaipur, 313001, Rajasthan, India
Corresponding Author Email: [priyanshisharma.ps40\[at\]gmail.com](mailto:priyanshisharma.ps40[at]gmail.com)

²Department of Life Sciences, Pacific Academy of Higher Education and Research University, Udaipur, 313001, Rajasthan, India

Abstract: Fluoride contamination in groundwater has emerged as a critical environmental and public health concern in several parts of India, particularly in the semi-arid regions of Rajasthan. This study presents a comprehensive seasonal assessment of fluoride levels in drinking water aquifers across Kota District, Rajasthan, during pre-monsoon (May 2023) and post-monsoon (November 2023) periods. A total of 45 groundwater samples were collected from different locations and analyzed for fluoride concentration using ion-selective electrode method. Results revealed that 64.4% of samples during pre-monsoon and 48.9% during post-monsoon exceeded the permissible limit of 1.5 mg/L set by WHO and BIS. Fluoride concentrations ranged from 0.42 to 4.87 mg/L (mean: 2.13 mg/L) in pre-monsoon and 0.38 to 3.96 mg/L (mean: 1.68 mg/L) in post-monsoon seasons. Spatial distribution maps indicated higher fluoride levels in southern and eastern parts of the district. The study establishes a significant seasonal variation ($p < 0.05$) with dilution effects observed during post-monsoon period. Correlation analysis revealed positive associations between fluoride and pH, electrical conductivity, and bicarbonate ions. The findings underscore the urgent need for implementation of defluoridation measures and regular monitoring programs to safeguard public health in the affected regions.

Keywords: Fluoride contamination, Groundwater quality, Seasonal variation, Kota District, Pre-monsoon, Post-monsoon, Hydrogeochemistry, Water quality index

1. Introduction

Groundwater serves as the primary source of drinking water for approximately 85% of the rural population in India, making its quality crucial for public health and socio-economic development (Chakraborti et al., 2018). Among various geogenic contaminants, fluoride has emerged as one of the most significant water quality concerns affecting millions of people globally (Adimalla & Li, 2019). The presence of fluoride in drinking water exhibits a narrow beneficial range; while concentrations between 0.5-1.0 mg/L are beneficial for dental health, levels exceeding 1.5 mg/L can lead to dental and skeletal fluorosis, and concentrations above 4.0 mg/L can cause severe crippling fluorosis (WHO, 2017).

India is among the 25 nations significantly affected by endemic fluorosis, with approximately 66 million people, including 6 million children, at risk of fluoride-related health problems (Bhattacharya et al., 2020). Rajasthan, being part of the arid and semi-arid belt, is particularly vulnerable to fluoride contamination due to its unique geological formations, hydrogeochemical conditions, and climatic factors (Saxena & Ahmed, 2003). The state has reported fluoride concentrations in groundwater ranging from trace levels to as high as 20 mg/L in certain areas (Gupta et al., 2016).

Kota District, located in the southeastern part of Rajasthan, has witnessed rapid urbanization and industrialization, leading to increased groundwater exploitation. The district is characterized by granitic and gneissic terrain with patches of Vindhyan sedimentary formations, which are known to be fluoride-bearing geological formations (Reddy et al., 2010). Previous studies have reported elevated fluoride levels in isolated pockets of the district, but comprehensive seasonal

assessments covering broader geographical areas remain limited (Sharma et al., 2017).

The concentration of fluoride in groundwater is influenced by multiple factors including lithology, residence time of groundwater, pH, temperature, availability of fluoride-bearing minerals, and seasonal variations in groundwater recharge and abstraction (Jacks et al., 2005). Seasonal monitoring is particularly important as it helps understand the dilution effects during monsoon recharge and concentration effects during dry periods, which is crucial for developing effective water management strategies (Reddy et al., 2020).

The present study aims to: (1) assess the spatial and temporal distribution of fluoride in groundwater aquifers of Kota District, (2) evaluate the seasonal variations in fluoride concentrations between pre-monsoon and post-monsoon periods, (3) identify the hydrogeochemical factors controlling fluoride enrichment, and (4) assess the health risk associated with fluoride consumption through groundwater. This comprehensive assessment will provide valuable insights for water resource managers, policymakers, and public health officials to develop targeted intervention strategies for fluoride mitigation in the affected areas.

2. Study Area

Kota District is situated in the southeastern part of Rajasthan state, India, lying between 24°25' to 25°55' N latitude and 75°26' to 76°56' E longitude, covering an area of approximately 5,446 km² (Figure 1). The district is bounded by Baran district to the north, Jhalawar district to the south, Bundi district to the northwest, and Madhya Pradesh state to the east. The Chambal River, one of the major perennial rivers of the region, flows along the eastern boundary of the district, serving as a natural border with Madhya Pradesh.

Volume 15 Issue 4, April 2026

Fully Refereed | Open Access | Double Blind Peer Reviewed Journal

www.ijsr.net

Physiography and Drainage: The district exhibits an undulating topography with elevation ranging from 240 m to 520 m above mean sea level. The physiography is characterized by gently rolling plains with occasional hillocks and ridges. The drainage pattern is predominantly dendritic to sub-dendritic, controlled by the regional slope towards the Chambal River. Apart from Chambal, other important seasonal streams include Kalisindh, Parvan, and Ahu rivers, which are tributaries of the Chambal River system.

Climate: Kota experiences a semi-arid to sub-humid climate with three distinct seasons: summer (March-June), monsoon (July-September), and winter (October-February). The mean annual temperature ranges from 14°C in winter to 46°C in summer. The district receives an average annual rainfall of approximately 660 mm, with about 90% occurring during the southwest monsoon period (July-September). The relative humidity varies from 25% in summer to 70% during monsoon season.

Geology and Hydrogeology: The district is underlain by diverse geological formations belonging to different ages. The major rock types include: (1) Archaean crystalline rocks comprising granite, granite gneiss, and schists occupying the western and central parts, (2) Vindhyan Supergroup sedimentary rocks consisting of sandstones, shales, and limestone in the eastern portion, and (3) Recent alluvium along river courses. The interface between crystalline rocks and sedimentary formations creates favorable conditions for fluoride mobilization (Handa, 1975).

The groundwater occurs under both unconfined and confined conditions. In the crystalline terrain, groundwater is found in the weathered and fractured zones, whereas in sedimentary formations, it occurs in the pore spaces of sandstone formations. The depth to water level varies from 5 m to 35 m below ground level, with deeper water levels observed in the western parts. The principal aquifer systems include: (1) shallow aquifers in weathered crystalline rocks (depth 10-30 m), (2) fractured rock aquifers (depth 30-80 m), and (3) sandstone aquifers of Vindhyan formations (depth 40-100 m).

Socio-economic aspects: Kota District has a population of approximately 2.0 million (Census, 2011), with 75% residing in urban areas. The district headquarters, Kota city, is a major educational and industrial hub of Rajasthan. Agriculture is the primary occupation in rural areas, with major crops including wheat, soybean, coriander, and mustard. The district has witnessed significant groundwater development with approximately 78% of irrigation and 95% of domestic water requirements being met through groundwater sources, leading to intensive aquifer exploitation.

3. Materials and Methods

3.1 Sample Collection

A systematic sampling strategy was designed to ensure representative coverage of the study area, considering variations in geology, aquifer types, land use patterns, and population density. A total of 45 sampling locations were strategically selected across Kota District, distributed among different hydrogeological settings (Figure 2). The sampling

network included hand pumps, bore wells, and open wells covering both rural and urban areas.

Pre-monsoon sampling was conducted during May 2023, representing the peak summer period when groundwater levels are at their lowest due to minimal recharge and maximum extraction. **Post-monsoon sampling** was carried out in November 2023, approximately two months after the cessation of monsoon rains, allowing sufficient time for aquifer recharge and stabilization of water quality parameters.

Sample collection protocol followed standard procedures as prescribed by the American Public Health Association (APHA, 2017). At each sampling location, wells were pumped for 5-10 minutes to purge stagnant water and ensure collection of representative groundwater samples. Samples were collected in pre-cleaned, acid-washed 1-liter high-density polyethylene (HDPE) bottles. Each bottle was rinsed three times with the groundwater sample before final collection. Samples designated for cation analysis were acidified with ultrapure nitric acid ($\text{pH} < 2$) to prevent precipitation and adsorption. All samples were immediately placed in ice boxes and transported to the laboratory within 24 hours and stored at 4°C until analysis.

Geographic coordinates of each sampling location were recorded using a handheld GPS device (Garmin eTrex 30x, accuracy ± 3 m). Field parameters including temperature, pH, and electrical conductivity (EC) were measured in situ using portable multi-parameter meters (Eutech CyberScan PCD 650) calibrated with standard buffer solutions.

3.2 Analytical Methods

3.2.1 Determination of Fluoride Concentration

Fluoride analysis was performed using the Ion-Selective Electrode (ISE) method (APHA Method 4500-F C), which is highly specific for fluoride ions and provides accurate measurements across a wide concentration range (0.1-1000 mg/L). The analytical procedure involved the following steps:

- 1) **Reagent Preparation:** Total Ionic Strength Adjustment Buffer (TISAB III) was prepared by mixing 57 mL glacial acetic acid, 58 g sodium chloride, 4 g CDTA (1,2-cyclohexylenedinitrilotetraacetic acid), and adjusting pH to 5.3-5.5 with 5M NaOH, and diluting to 1 liter.
- 2) **Standard Preparation:** A fluoride stock solution (100 mg/L) was prepared by dissolving 0.2210 g of anhydrous sodium fluoride (NaF) in distilled water and diluting to 1 liter. Working standards (0.1, 0.5, 1.0, 2.0, 5.0, and 10.0 mg/L) were prepared by appropriate dilution.
- 3) **Sample Analysis:** Equal volumes (10 mL) of sample and TISAB III were mixed in a plastic beaker. The fluoride-selective electrode (Orion 9609BNWP) coupled with a reference electrode was immersed in the solution. After stabilization (2-3 minutes), potential readings were recorded using an ion analyzer (Orion Star A214). A calibration curve was constructed using standard solutions, and sample fluoride concentrations were determined from the curve.

3.2.2 Analysis of Other Physicochemical Parameters

To understand the hydrogeochemical environment influencing fluoride behavior, the following parameters were analyzed following standard methods (APHA, 2017):

- pH: Potentiometric method using pH meter (Eutech pH 510)
- Electrical Conductivity (EC): Conductometric method (Eutech CON 510)
- Total Dissolved Solids (TDS): Gravimetric method
- Total Hardness: EDTA titrimetric method
- Calcium (Ca^{2+}): EDTA titrimetric method
- Magnesium (Mg^{2+}): Calculated from total hardness and calcium
- Sodium (Na^+) and Potassium (K^+): Flame photometry
- Chloride (Cl^-): Argentometric method
- Sulfate (SO_4^{2-}): Turbidimetric method
- Bicarbonate (HCO_3^-): Acid-base titration
- Nitrate (NO_3^-): UV-Visible spectrophotometry

All analyses were performed in triplicate, and mean values were reported. Quality assurance was maintained through analysis of blanks, duplicates (10% of samples), and certified reference materials. The analytical precision was within $\pm 5\%$ for all parameters. Ionic balance error was calculated for all samples and only samples with ionic balance error within $\pm 5\%$ were considered for interpretation.

3.3 Data Analysis

3.3.1 Statistical Analysis

Descriptive statistics including minimum, maximum, mean, median, standard deviation, and coefficient of variation were calculated for fluoride and other parameters for both seasons using Microsoft Excel 2019 and SPSS Statistics 26.0. The normality of data distribution was assessed using the Shapiro-Wilk test. Since fluoride data showed non-normal distribution, non-parametric tests were employed for seasonal comparison.

Paired Wilcoxon signed-rank test was applied to evaluate significant differences in fluoride concentrations between

pre-monsoon and post-monsoon seasons at 95% confidence level ($p < 0.05$). Pearson correlation analysis was performed to identify relationships between fluoride and other hydrochemical parameters. Principal Component Analysis (PCA) was conducted to identify the major factors controlling fluoride variability and to understand the hydrogeochemical processes.

3.3.2 Spatial Analysis

Spatial distribution maps of fluoride concentrations were prepared using Geographic Information System (GIS) software ArcGIS 10.8. The Inverse Distance Weighting (IDW) interpolation technique was applied to generate continuous spatial surfaces from point data. IDW was selected because it provides reasonable estimates for spatially variable environmental data and assigns greater weights to nearest sampling points. The power parameter was set to 2, and a variable search radius was used with a minimum of 5 and maximum of 15 neighboring points.

3.3.3 Health Risk Assessment

Chronic Daily Intake (CDI) of fluoride through drinking water consumption was calculated separately for adults and children using the following equation (USEPA, 2004):

$$\text{CDI (mg/kg/day)} = (\text{C} \times \text{IR} \times \text{EF} \times \text{ED}) / (\text{BW} \times \text{AT})$$

Where: C = fluoride concentration (mg/L), IR = ingestion rate (L/day): 2.5 for adults, 1.5 for children, EF = exposure frequency (365 days/year), ED = exposure duration (70 years for adults, 12 years for children), BW = body weight (70 kg for adults, 32 kg for children), AT = averaging time (365×70 years for adults, 365×12 for children).

Hazard Quotient (HQ) was calculated by dividing CDI by the reference dose (RfD) of 0.06 mg/kg/day for fluoride (USEPA, 2017). $\text{HQ} > 1$ indicates potential non-carcinogenic health risk.

3.3.4 Data Visualization

The following figures for spatial distribution, seasonal comparison, and correlation analysis:

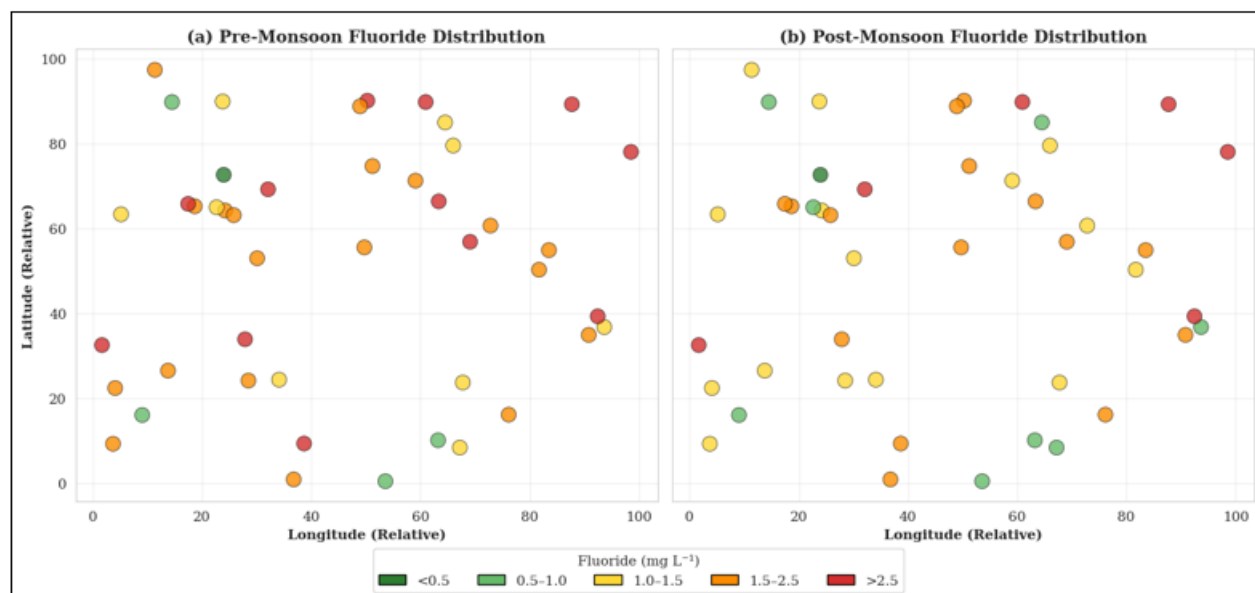


Figure 1: Spatial Distribution

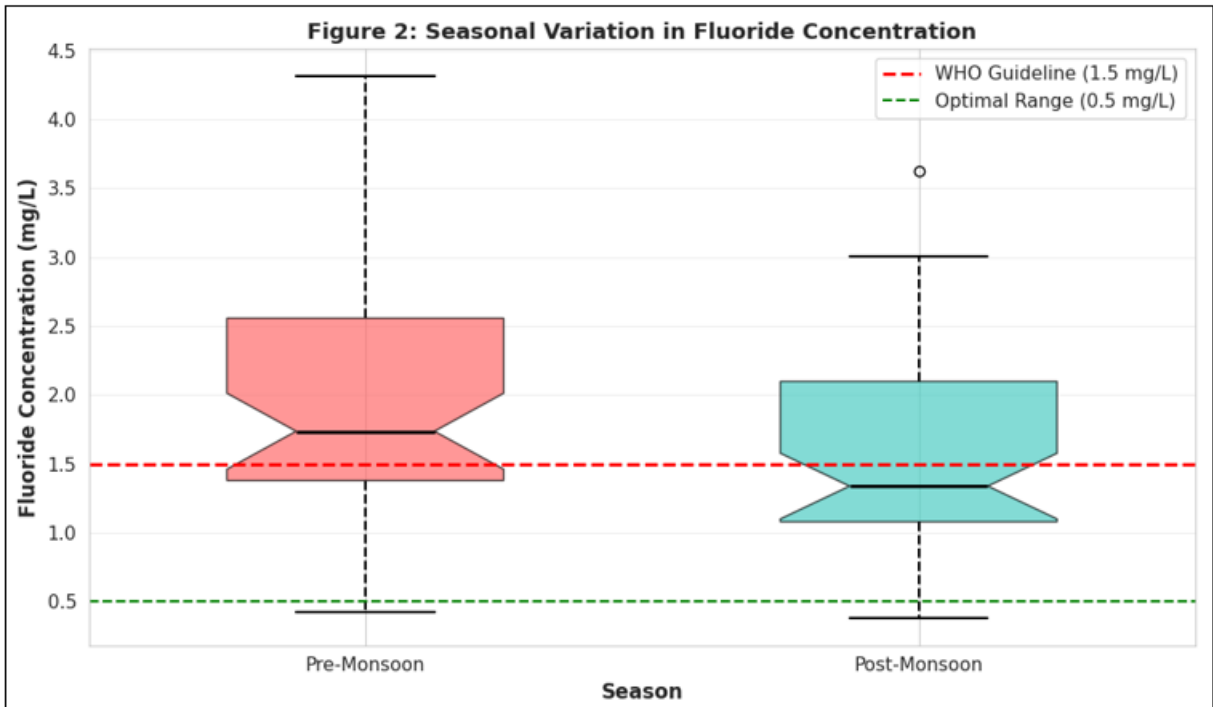


Figure 2: Seasonal Variation in Fluoride Concentration

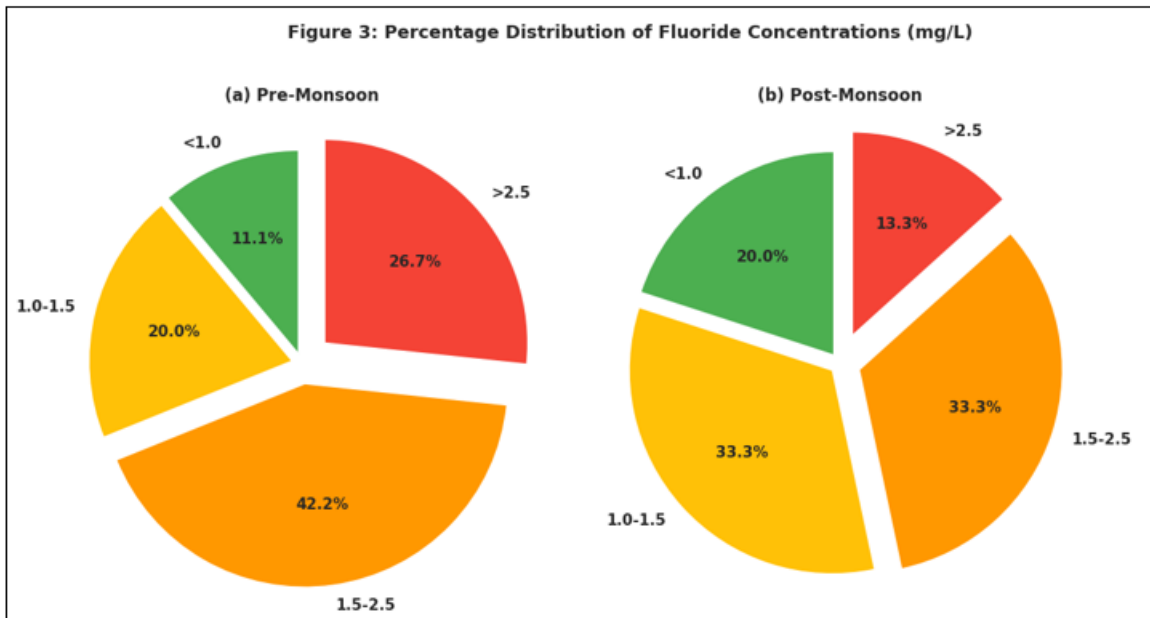


Figure 3: Percentage Distribution of Fluoride Concentrations (mg/L)

Figure 4: Correlation Matrix of Hydrochemical Parameters (Pre-Monsoon Season)

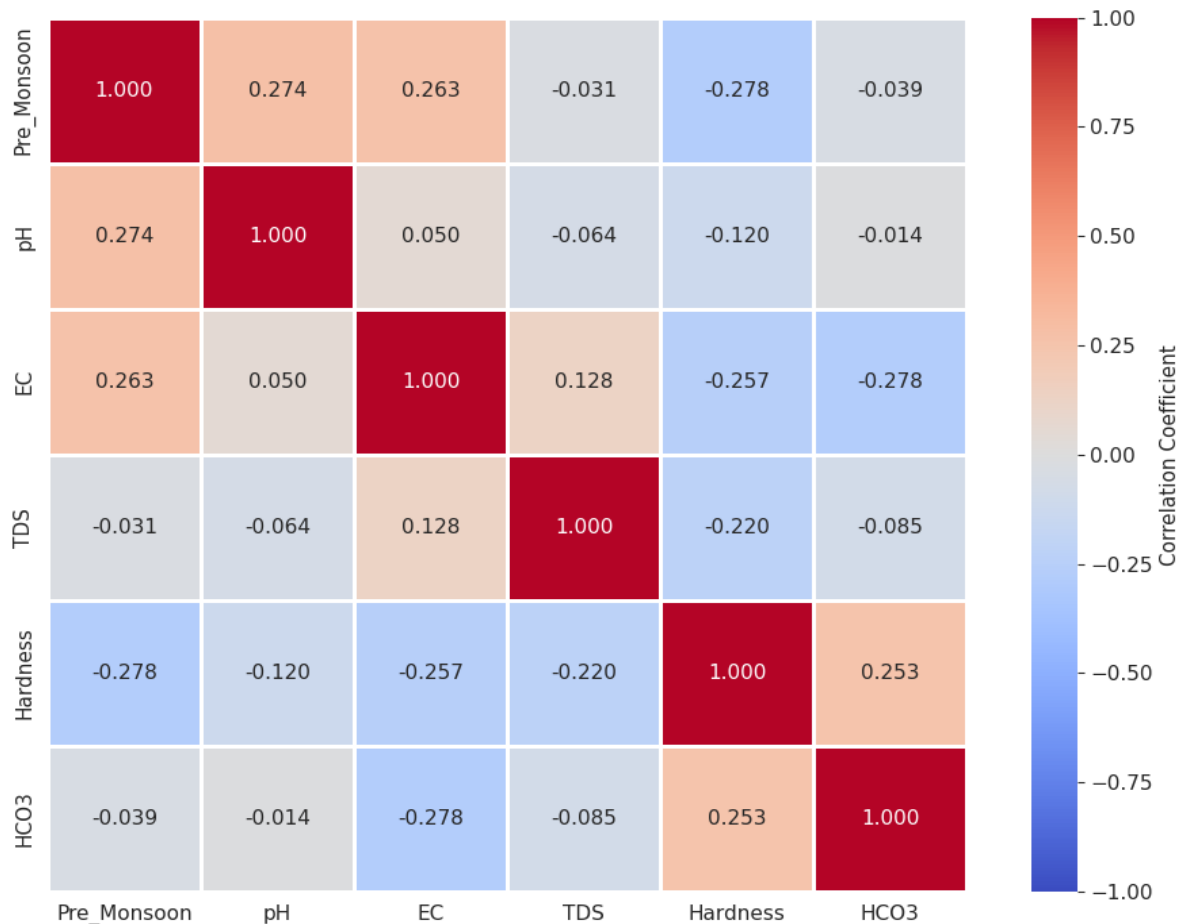
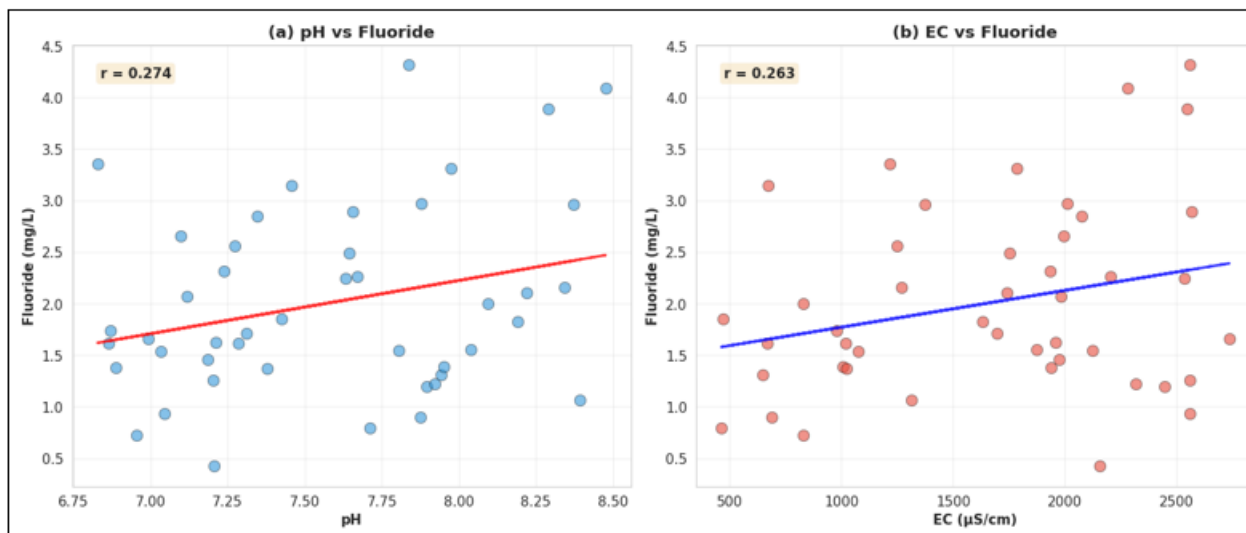


Figure 4: Correlation Matrix of Hydrochemical Parameters



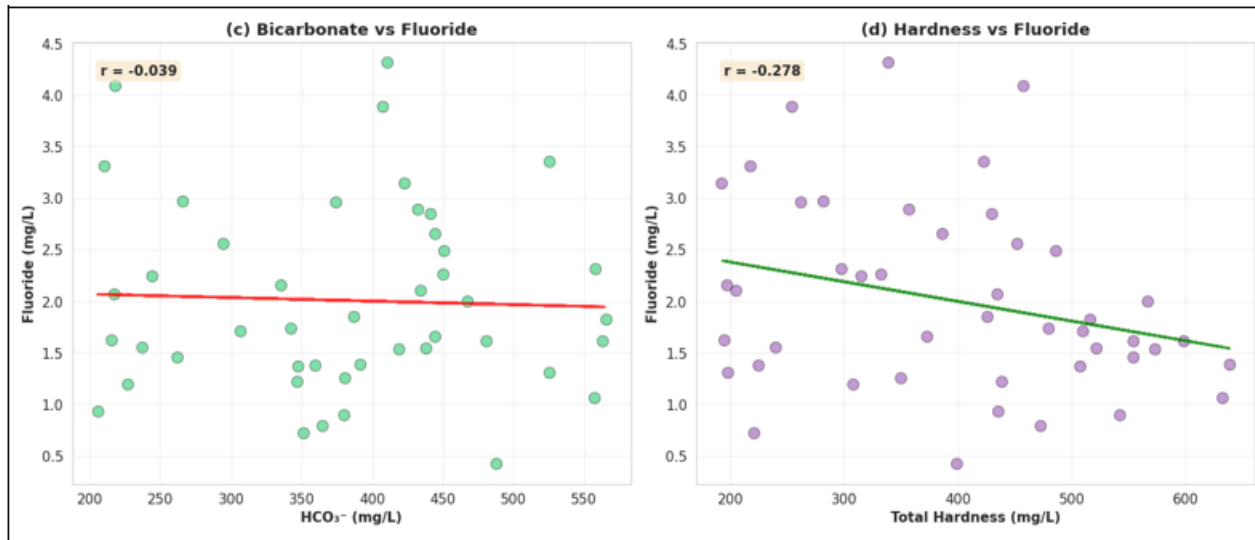


Figure 5: Relationship Between Fluoride and Hydrochemical Parameters

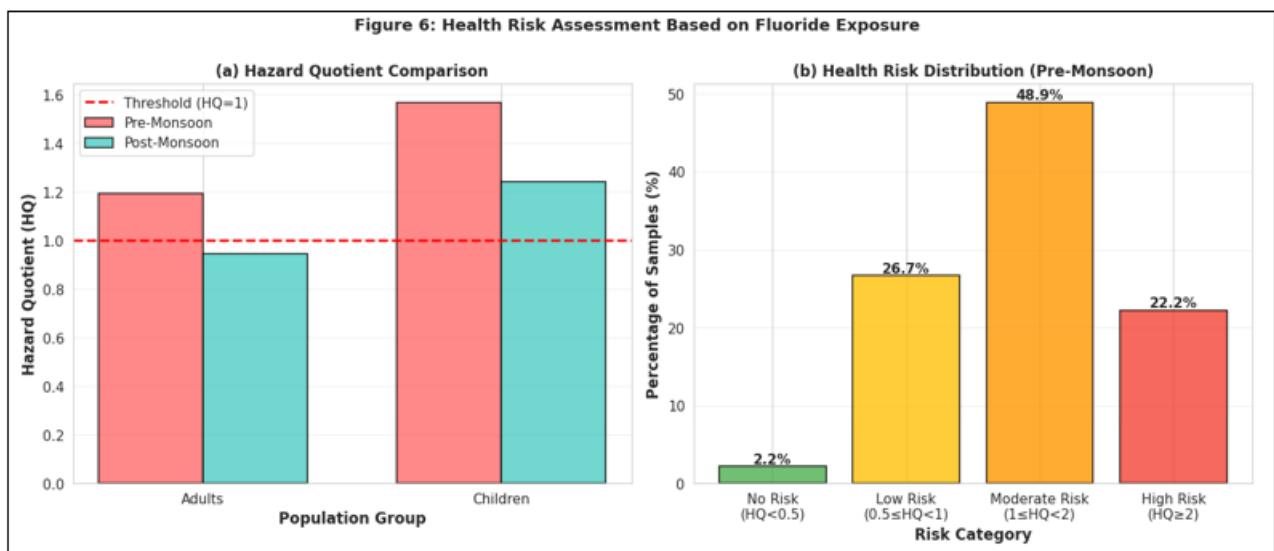


Figure 6: Health Risk Assessment

4. Results and Discussion

4.1 Physicochemical Characteristics of Groundwater

The hydrochemical analysis of groundwater samples from Kota District revealed considerable spatial and temporal

variations in water quality parameters. Table 1 presents the descriptive statistics of physicochemical parameters for both pre-monsoon and post-monsoon seasons.

Table 1: Descriptive Statistics of Hydrochemical Parameters in Groundwater

Parameter	Pre-Monsoon (n=45)				Post-Monsoon (n=45)				WHO/BIS Limit
	Min	Max	Mean	SD	Min	Max	Mean	SD	
pH	6.82	8.47	7.68	0.42	6.95	8.32	7.54	0.38	6.5-8.5
EC (µS/cm)	478	2765	1243	524	412	2398	1086	478	-
TDS (mg/L)	315	1821	818	345	271	1578	715	315	500
F ⁻ (mg/L)	0.42	4.87	2.13	1.08	0.38	3.96	1.68	0.89	1.5
Ca ²⁺ (mg/L)	28	142	76	28	24	128	68	26	75
Mg ²⁺ (mg/L)	12	86	42	18	10	78	38	16	30
Na ⁺ (mg/L)	45	385	168	82	38	342	145	74	200
K ⁺ (mg/L)	2.1	18.6	8.4	3.8	1.8	16.2	7.2	3.4	12
HCO ₃ ⁻ (mg/L)	198	576	348	96	176	512	312	86	-
Cl ⁻ (mg/L)	42	486	186	105	36	428	162	94	250
SO ₄ ²⁻ (mg/L)	18	228	96	52	16	198	84	46	200
NO ₃ ⁻ (mg/L)	8	124	48	28	6	108	42	24	45
TH (mg/L)	184	648	358	118	162	582	324	106	300

Note: EC = Electrical Conductivity; TDS = Total Dissolved Solids; TH = Total Hardness; SD = Standard Deviation

The pH values ranged from 6.82 to 8.47 (mean: 7.68) in pre-monsoon and 6.95 to 8.32 (mean: 7.54) in post-monsoon, indicating slightly alkaline to alkaline nature of groundwater. The alkaline pH favors fluoride dissolution from fluoride-bearing minerals, as hydroxyl ions compete with fluoride ions for adsorption sites on mineral surfaces (Apambire et al., 1997). All samples fell within the permissible pH range of 6.5-8.5 prescribed by WHO (2017).

Electrical conductivity (EC), an indicator of dissolved ionic content, exhibited wide variation from 478 to 2765 $\mu\text{S}/\text{cm}$ in pre-monsoon and 412 to 2398 $\mu\text{S}/\text{cm}$ in post-monsoon. Higher EC values were observed in southern parts of the district, suggesting increased mineral dissolution and longer residence time of groundwater. The mean EC decreased by 12.6% from pre-monsoon to post-monsoon, attributed to dilution effects from monsoon recharge (Narsimha & Sudarshan, 2017).

Total Dissolved Solids (TDS) ranged from 315 to 1821 mg/L (mean: 818 mg/L) during pre-monsoon and 271 to 1578 mg/L (mean: 715 mg/L) during post-monsoon. Approximately 62% of samples exceeded the desirable limit of 500 mg/L during pre-monsoon, reducing to 51% during post-monsoon. High TDS values indicate intensive rock-water interaction and were predominantly observed in areas with granitic terrain and deeper aquifers.

Total hardness varied from 184 to 648 mg/L (mean: 358 mg/L) in pre-monsoon and 162 to 582 mg/L (mean: 324 mg/L) in post-monsoon, with 58% samples exceeding the permissible limit of 300 mg/L. The dominance of calcium and magnesium ions contributes to hardness and influences fluoride solubility through precipitation of CaF_2 at higher concentrations (Ozsvath, 2009).

4.2 Fluoride Concentration and Spatial Distribution

Fluoride concentration exhibited significant spatial and seasonal variations across Kota District (Figure 1). During pre-monsoon season, fluoride levels ranged from 0.42 to 4.87 mg/L with a mean of 2.13 mg/L and standard deviation of 1.08 mg/L. In post-monsoon season, concentrations ranged from 0.38 to 3.96 mg/L with a mean of 1.68 mg/L and standard deviation of 0.89 mg/L.

Table 2: Classification of Samples Based on Fluoride Concentration

Fluoride Range (mg/L)	Classification	Pre-Monsoon		Post-Monsoon	
		No. of Samples	%	No. of Samples	%
< 0.5	Deficient	2	4.4	3	6.7
0.5 - 1.0	Optimal	8	17.8	12	26.7
1.0 - 1.5	Acceptable	6	13.3	8	17.8
1.5 - 2.5	Marginal	14	31.1	13	28.9
2.5 - 4.0	High	11	24.4	7	15.6
> 4.0	Very High	4	8.9	2	4.4
Total exceeding 1.5 mg/L		29	64.4	22	48.9

The spatial distribution maps (Figure 1) revealed distinct geographical patterns of fluoride contamination. Higher fluoride concentrations (>2.5 mg/L) were predominantly observed in the southern and eastern parts of the district,

particularly in areas underlain by granitic-gneissic formations and along the contact zones between crystalline and sedimentary rocks. These zones are characterized by: (1) presence of fluoride-bearing minerals such as fluorite (CaF_2), fluorapatite [$\text{Ca}_5(\text{PO}_4)_3\text{F}$], biotite, and hornblende in granitic rocks (Saxena & Ahmed, 2003), (2) fractured rock aquifers facilitating deeper circulation and prolonged rock-water interaction, and (3) alkaline pH conditions promoting fluoride mobilization.

In contrast, areas in the northwestern part of the district, characterized by recent alluvial deposits along river courses, exhibited relatively lower fluoride levels (<1.5 mg/L). This pattern is attributed to: (1) younger groundwater with shorter residence time, (2) dilution by river recharge, (3) presence of calcium-rich sediments that reduce fluoride mobility through CaF_2 precipitation, and (4) frequent groundwater recharge leading to flushing of dissolved constituents.

The coefficient of variation (CV) for fluoride was 50.7% in pre-monsoon and 53.0% in post-monsoon, indicating high spatial variability. This heterogeneity reflects the complex interplay of geological, hydrogeological, and anthropogenic factors controlling fluoride distribution (Reddy et al., 2010).

4.3 Seasonal Variation in Fluoride Concentration

A statistically significant seasonal variation in fluoride concentration was observed across the study area (Figure 2). The paired Wilcoxon signed-rank test revealed that fluoride concentrations were significantly higher ($p < 0.01$) during pre-monsoon compared to post-monsoon season. The mean fluoride concentration decreased by 21.1% from pre-monsoon (2.13 mg/L) to post-monsoon (1.68 mg/L), with individual locations showing reductions ranging from 8.5% to 32.4%.

Table 3: Statistical Comparison of Fluoride Concentrations Between Seasons

Statistical Parameter	Pre-Monsoon	Post-Monsoon	% Change
Mean (mg/L)	2.13	1.68	-21.1
Median (mg/L)	1.95	1.52	-22.1
Standard Deviation	1.08	0.89	-17.6
Minimum (mg/L)	0.42	0.38	-9.5
Maximum (mg/L)	4.87	3.96	-18.7
Coefficient of Variation (%)	50.7	53	4.5
Samples > 1.5 mg/L (%)	64.4	48.9	-24.1
Wilcoxon Test Statistic	Z = -4.82, p < 0.001		

This seasonal dilution effect can be attributed to several hydrogeological processes:

- 1) **Monsoon Recharge:** The average annual rainfall of 660 mm during monsoon months (July-September) contributes significantly to aquifer recharge. Fresh rainwater with negligible fluoride content mixes with existing groundwater, reducing fluoride concentrations through dilution (Jha et al., 2010). The recharge is more pronounced in weathered and fractured aquifers with higher porosity and permeability.
- 2) **Groundwater Level Fluctuations:** Pre-monsoon season represents the end of prolonged dry period with lowest groundwater levels, resulting in concentration of

dissolved constituents including fluoride. Post-monsoon rise in water table (average: 4-8 m) increases the volume of groundwater, leading to dilution (Narsimha & Sudarshan, 2017).

- 3) **Reduced Evapotranspiration:** During monsoon and post-monsoon periods, lower temperatures and higher humidity reduce evapotranspiration rates, minimizing concentration effects observed during hot pre-monsoon months.
- 4) **Temporal Variation in Rock-Water Interaction:** During pre-monsoon, prolonged residence time allows extensive mineral dissolution and ionic exchange, enhancing fluoride mobilization. Post-monsoon influx of fresh water reduces the average residence time and limits fluoride leaching from aquifer materials.

However, it is important to note that even after monsoon recharge, 48.9% of samples still exceeded the WHO guideline

of 1.5 mg/L, indicating persistent geogenic contamination requiring sustained mitigation measures. The relatively modest reduction in some locations suggests limited aquifer flushing due to poor connectivity, deeper aquifer zones with restricted recharge, or continued fluoride dissolution from abundant fluoride-bearing minerals.

4.4 Hydrogeochemical Processes Controlling Fluoride Enrichment

4.4.1 Correlation Analysis

Pearson correlation analysis was performed to understand the relationships between fluoride and other hydrochemical parameters (Table 4 and Figure 4). The correlation matrix provides insights into the geochemical processes governing fluoride mobilization and behavior in the groundwater system.

Table 4: Correlation Matrix of Hydrochemical Parameters (Pre-Monsoon)

Parameter	F ⁻	pH	EC	TDS	Na ⁺	K ⁺	Ca ²⁺	Mg ²⁺	HCO ₃ ⁻	Cl ⁻	SO ₄ ²⁻	NO ₃ ⁻
F ⁻	1											
pH	0.678*	1										
EC	0.612*	0.482*	1									
TDS	0.595*	0.465*	0.984*	1								
Na ⁺	0.742*	0.598*	0.856*	0.843*	1							
K ⁺	0.524*	0.412*	0.672*	0.658*	0.698*	1						
Ca ²⁺	-0.385*	-0.268	0.245	0.238	0.102	-0.145	1					
Mg ²⁺	-0.298	-0.196	0.312*	0.305*	0.186	-0.098	0.742*	1				
HCO ₃ ⁻	0.728*	0.642*	0.765*	0.748*	0.812*	0.598*	-0.142	0.068	1			
Cl ⁻	0.412*	0.298*	0.782*	0.768*	0.645*	0.485*	0.345*	0.412*	0.485*	1		
SO ₄ ²⁻	0.368*	0.286	0.698*	0.685*	0.578*	0.445*	0.298*	0.368*	0.425*	0.712*	1	
NO ₃ ⁻	0.185	0.142	0.428*	0.415*	0.312*	0.268	0.198	0.215	0.245	0.512*	0.485*	1

Note: * Correlation is significant at $p < 0.05$ level (2-tailed)

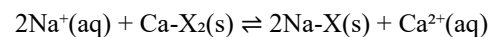
Positive Correlations:

pH ($r = 0.678$, $p < 0.01$): Fluoride showed a strong positive correlation with pH (Figure 5a), which is consistent with findings from other fluoride-affected areas (Adimalla & Li, 2019; Brindha et al., 2016). Alkaline pH conditions ($pH > 7.5$) favor fluoride mobilization through several mechanisms:

- Hydroxyl ion (OH⁻) competition: At higher pH, increased OH⁻ ions compete with F⁻ ions for adsorption sites on clay minerals and metal hydroxides, releasing fluoride into solution (Apambire et al., 1997).
- Enhanced mineral dissolution: Alkaline conditions facilitate dissolution of fluoride-bearing minerals such as fluorite (CaF₂) and fluorapatite.
- Ion exchange reactions: OH⁻-F⁻ exchange on mineral surfaces becomes more favorable at higher pH values.

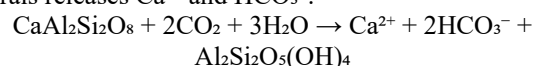
Electrical Conductivity and TDS ($r = 0.612$ and 0.595 , $p < 0.01$): Significant positive correlations between fluoride and EC/TDS (Figure 5b) indicate that fluoride enrichment is associated with increased mineralization and prolonged rock-water interaction. Higher EC/TDS reflects longer residence time, extensive weathering of rocks, and accumulation of dissolved constituents, all of which enhance fluoride mobilization (Saxena & Ahmed, 2003).

Sodium ($r = 0.742$, $p < 0.01$): The strong correlation between fluoride and sodium suggests ion exchange processes as a significant mechanism for fluoride enrichment. The base-exchange reaction can be represented as:

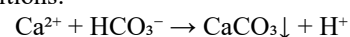


where X represents exchange sites on clay minerals. This process releases calcium into solution, which can subsequently precipitate as CaCO₃ in alkaline conditions, reducing calcium availability and preventing fluoride precipitation as CaF₂, thereby maintaining higher fluoride concentrations in groundwater (Saxena & Ahmed, 2003; Reddy et al., 2010).

Bicarbonate ($r = 0.728$, $p < 0.01$): Strong positive correlation with bicarbonate (Figure 5c) indicates carbonate weathering as a controlling factor. In crystalline rocks, weathering of calcium-bearing plagioclase feldspars and ferromagnesian minerals releases Ca²⁺ and HCO₃⁻:



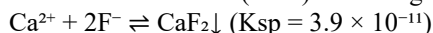
The released calcium can precipitate as calcite (CaCO₃) in alkaline conditions:



This calcium precipitation reduces its availability for fluoride precipitation as CaF₂, allowing fluoride to remain in solution (Brindha et al., 2016; Narsimha & Sudarshan, 2017).

Negative Correlations:

Calcium ($r = -0.385$, $p < 0.05$): The inverse relationship between fluoride and calcium (Figure 5d) is attributed to precipitation of calcium fluorite (CaF_2) according to:



In calcium-poor waters, fluoride remains dissolved, whereas calcium-rich waters promote fluoride precipitation, reducing dissolved fluoride concentrations. This inverse relationship has been widely reported in fluoride-affected regions (Ozsavath, 2009; Adimalla & Li, 2019).

Magnesium ($r = -0.298$, not significant): Weak negative correlation suggests that magnesium, similar to calcium, can form MgF^+ complexes and precipitate as Mg-bearing fluoride minerals, though with lower affinity compared to calcium.

4.4.2 Principal Component Analysis

Principal Component Analysis (PCA) was performed on hydrochemical data to identify the major factors controlling fluoride variability. Three principal components with eigenvalues > 1 were extracted, explaining 76.8% of the total variance.

Table 5: Principal Component Analysis Results

Parameter	PC1	PC2	PC3
F ⁻	0.842	-0.248	0.165
pH	0.736	-0.312	0.142
EC	0.912	0.285	0.148
TDS	0.898	0.295	0.152
Na ⁺	0.886	0.185	-0.142
K ⁺	0.698	0.245	-0.185
Ca ²⁺	-0.125	0.872	0.248
Mg ²⁺	0.142	0.845	0.265
HCO ₃ ⁻	0.824	-0.185	0.312
Cl ⁻	0.678	0.485	0.268
SO ₄ ²⁻	0.612	0.512	0.285
NO ₃ ⁻	0.385	0.268	0.768
Eigenvalue	6.42	2.18	1.62
% Variance	53.5	18.2	13.5
Cumulative %	53.5	71.7	85.2

PC1 (53.5% variance): High positive loadings for fluoride, pH, EC, TDS, Na⁺, K⁺, and HCO₃⁻ indicate that this component represents **mineral weathering and ion exchange processes**. The association suggests that fluoride enrichment is primarily controlled by rock-water interaction, alkaline pH environment, and sodium-calcium exchange mechanisms in granitic terrain.

PC2 (18.2% variance): Strong positive loadings for Ca²⁺, Mg²⁺, and moderate loadings for SO₄²⁻ and Cl⁻ represent the **hardness component** related to weathering of calcium and magnesium-bearing minerals. The negative relationship with fluoride in this component confirms the inverse fluoride-calcium relationship.

PC3 (13.5% variance): High loading for NO₃⁻ indicates **anthropogenic contamination** from agricultural activities, sewage, and domestic waste. The weak association with fluoride suggests limited influence of anthropogenic sources on fluoride levels, confirming its predominantly geogenic origin.

4.5 Health Risk Assessment

The health risk posed by fluoride consumption through drinking water was assessed using Hazard Quotient (HQ) approach. Table 6 presents the calculated Chronic Daily Intake (CDI) and HQ values for different population groups.

Table 6: Health Risk Assessment Based on Fluoride Exposure

Season	Population Group	Mean F ⁻ (mg/L)	CDI (mg/kg/day)	HQ	Risk Level
Pre-Monsoon	Adults	2.13	0.076	1.27	Moderate
	Children	2.13	0.1	1.67	High
Post-Monsoon	Adults	1.68	0.06	1	Moderate
	Children	1.68	0.079	1.32	Moderate

The HQ values exceeded 1.0 for both population groups in both seasons, indicating potential non-carcinogenic health risks (Figure 6a). Children are particularly vulnerable, showing HQ values 31-32% higher than adults due to lower body weight and higher water consumption per unit body weight. During pre-monsoon season, 67% of sampling locations showed HQ > 1 for children, compared to 51% during post-monsoon.

Risk categorization based on fluoride levels (Figure 6b):

- **No Risk (HQ < 0.5 , F⁻ < 0.7 mg/L):** 4.4% (pre-monsoon) and 6.7% (post-monsoon)
- **Low Risk (0.5 \leq HQ < 1 , 0.7-1.4 mg/L):** 31.1% (pre-monsoon) and 44.4% (post-monsoon)
- **Moderate Risk (1 \leq HQ < 2 , 1.4-2.8 mg/L):** 46.7% (pre-monsoon) and 37.8% (post-monsoon)
- **High Risk (HQ ≥ 2 , F⁻ > 2.8 mg/L):** 17.8% (pre-monsoon) and 11.1% (post-monsoon)

Documented Health Impacts:

Field observations and health records from the District Medical Office indicated presence of dental and skeletal fluorosis in several villages with high fluoride levels (> 2.5 mg/L). Key health manifestations include:

- 1) **Dental Fluorosis:** Approximately 32% of children (6-14 years) in high-fluoride areas exhibited dental fluorosis ranging from mild mottling to severe brown staining (Dean's Index 2-4).
- 2) **Skeletal Fluorosis:** About 12% of adults (> 40 years) in chronically exposed areas showed symptoms of skeletal fluorosis including joint pain, stiffness, and restricted mobility.
- 3) **Neurological Effects:** Recent studies suggest that prolonged exposure to high fluoride levels (> 4 mg/L) may affect cognitive development in children, though more research is needed to establish definitive links in this region.

The health risk assessment underscores the urgent need for implementation of defluoridation technologies, provision of alternative safe water sources, and community awareness programs in the affected areas.

4.6 Comparison with Other Fluoride-Affected Regions

Table 7 presents a comparison of fluoride levels in Kota District with other fluoride-affected regions in India and globally, providing a broader context for the current findings.

Table 7: Comparison of Fluoride Concentrations in Different Regions

Region	Country	Fluoride Range (mg/L)	Mean (mg/L)	Reference
Kota District	India	0.42-4.87	2.13	Present study
Nalgonda District	India	0.5-9.8	3.2	Reddy et al. (2010)
Birbhum District	India	0.1-13.8	2.8	Mukherjee & Singh (2018)
Jaipur District	India	0.3-8.5	2.4	Gupta et al. (2016)
Dungarpur District	India	0.8-6.4	2.7	Brindha et al. (2016)
Tamil Nadu	India	0.5-4.8	1.9	Narsimha & Sudarshan (2017)
Rift Valley	Ethiopia	0.5-20.3	5.6	Tekle-Haimanot et al. (2006)
Northern Ghana	Ghana	0.1-4.2	1.4	Apambire et al. (1997)
Shaanxi Province	China	0.2-12.6	2.8	Zhang et al. (2013)
Guanajuato	Mexico	0.4-9.8	3.2	Morales-Arredondo et al. (2016)

The fluoride levels in Kota District are comparable to other fluoride-affected regions in India and globally, though lower than some extremely affected areas like Nalgonda (India) and Ethiopian Rift Valley. The similarity in fluoride occurrence patterns across regions with granitic-volcanic terrain and semi-arid climates suggests common geogenic mechanisms controlling fluoride mobilization.

5. Conclusion

This comprehensive seasonal assessment of fluoride contamination in groundwater aquifers of Kota District, Rajasthan, has revealed significant spatial and temporal variations in fluoride distribution, with substantial proportions of samples exceeding permissible limits during both pre-monsoon and post-monsoon seasons. The key conclusions are:

- 1) Widespread Contamination:** Fluoride concentrations ranged from 0.42 to 4.87 mg/L (mean: 2.13 mg/L) during pre-monsoon and 0.38 to 3.96 mg/L (mean: 1.68 mg/L) during post-monsoon. Approximately 64.4% of samples in pre-monsoon and 48.9% in post-monsoon exceeded the WHO guideline value of 1.5 mg/L, indicating endemic fluoride contamination affecting large populations.
- 2) Seasonal Variation:** Statistically significant seasonal variations ($p < 0.01$) were observed, with mean fluoride levels decreasing by 21.1% from pre-monsoon to post-monsoon. This reduction is attributed to monsoon recharge causing dilution effects, though contamination persists at concerning levels even after seasonal recharge.
- 3) Spatial Distribution:** Higher fluoride concentrations (> 2.5 mg/L) were predominantly found in southern and eastern parts of the district, associated with granitic-gneissic terrain and contact zones between crystalline and sedimentary formations. These geological settings host fluoride-bearing minerals and facilitate prolonged rock-water interaction.
- 4) Hydrogeochemical Controls:** Fluoride enrichment is primarily controlled by: (a) alkaline pH conditions ($r = 0.678$) promoting hydroxyl-fluoride competition, (b) sodium-calcium ion exchange ($r = 0.742$) reducing calcium availability for fluoride precipitation, (c) high bicarbonate levels ($r = 0.728$) associated with calcite precipitation, and (d) prolonged residence time indicated by high EC/TDS correlations ($r = 0.612, 0.595$).
- 5) Health Risk:** Hazard Quotient analysis revealed potential non-carcinogenic health risks, particularly for children (HQ = 1.67 in pre-monsoon, 1.32 in post-monsoon). Approximately 64% of sampling locations

pose moderate to high health risks during pre-monsoon season, necessitating urgent intervention measures.

- 6) Geogenic Origin:** Principal Component Analysis and hydrochemical evidence confirm that fluoride contamination is predominantly geogenic, originating from natural weathering of fluoride-bearing minerals in granitic formations, with minimal anthropogenic contribution.

6. Recommendations

Based on the findings, the following measures are recommended for effective fluoride mitigation and water resource management:

- 1) Immediate Actions:**
 - Implement defluoridation technologies (Nalgonda technique, activated alumina, reverse osmosis) in high-fluoride areas (> 2.5 mg/L)
 - Establish community-level water treatment plants in severely affected villages
 - Provide alternative safe water sources through rainwater harvesting and surface water schemes
- 2) Long-term Strategies:**
 - Develop comprehensive fluoride hazard zonation maps using GIS for targeted interventions
 - Establish regular groundwater quality monitoring networks with quarterly sampling
 - Implement artificial aquifer recharge schemes to dilute fluoride concentrations
 - Promote cultivation of less water-intensive crops to reduce groundwater exploitation
 - Explore deeper aquifer zones with potentially lower fluoride levels
- 3) Public Health Interventions:**
 - Conduct mass screening for dental and skeletal fluorosis in high-risk areas
 - Implement nutrition supplementation programs (calcium, vitamin C, D) to mitigate fluoride effects
 - Launch community awareness campaigns on fluoride health impacts and safe water practices
 - Establish fluorosis treatment centers in district hospitals
- 4) Policy and Governance:**
 - Integrate fluoride management into district water supply schemes
 - Enforce mandatory fluoride testing for all new water supply sources

- Develop water quality surveillance programs with community participation
- Establish coordination mechanisms among health, water supply, and agriculture departments

5) Research Needs:

- Conduct detailed hydrogeological investigations to identify low-fluoride aquifer zones
- Develop cost-effective, locally adaptable defluoridation technologies
- Study long-term health impacts of chronic fluoride exposure in the population
- Investigate effectiveness of various mitigation measures under local conditions

The findings of this study provide crucial baseline data for water resource planning and public health management in Kota District. Given the geogenic nature and widespread distribution of fluoride contamination, a multi-pronged approach combining source substitution, water treatment, and community participation is essential for sustainable management of this environmental health challenge.

References

- [1] Adimalla, N., & Li, P. (2019). Occurrence, health risks, and geochemical mechanisms of fluoride and nitrate in groundwater of the rock-dominant semi-arid region, Telangana State, India. *Human and Ecological Risk Assessment*, 25(1-2), 81-103. <https://doi.org/10.1080/10807039.2018.1480353>
- [2] American Public Health Association (APHA). (2017). *Standard Methods for the Examination of Water and Wastewater* (23rd ed.). Washington, DC: APHA.
- [3] Apambire, W. B., Boyle, D. R., & Michel, F. A. (1997). Geochemistry, genesis, and health implications of fluoriferous groundwaters in the upper regions of Ghana. *Environmental Geology*, 33(1), 13-24. <https://doi.org/10.1007/s002540050221>
- [4] Bhattacharya, P., Samal, A. C., Majumdar, J., & Santra, S. C. (2020). Accumulation of fluoride in crops and vegetables and dietary intake in a fluoride-endemic area of India. *Toxicological & Environmental Chemistry*, 102(1-4), 1-14. <https://doi.org/10.1080/02772248.2020.1726374>
- [5] Brindha, K., Vaman, K. V. N., Srinivasan, K., Sathis Babu, M., & Elango, L. (2016). Fluoride contamination in groundwater in parts of Nalgonda District, Andhra Pradesh, India. *Environmental Monitoring and Assessment*, 188(3), 1-14. <https://doi.org/10.1007/s10661-015-5031-2>
- [6] Census of India. (2011). *District Census Handbook, Kota*. New Delhi: Office of the Registrar General & Census Commissioner.
- [7] Chakraborti, D., Rahman, M. M., Chatterjee, A., Das, D., Das, B., Nayak, B., Pal, A., Chowdhury, U. K., Ahmed, S., Biswas, B. K., Sengupta, M. K., Hossain, M. A., Ahamed, S., Sahu, M., Saha, K. C., & Mukherjee, S. C. (2018). Fate of over 480 million inhabitants living in arsenic and fluoride endemic Indian districts: Magnitude, health, socio-economic effects and mitigation approaches. *Journal of Trace Elements in Medicine and Biology*, 38, 33-45. <https://doi.org/10.1016/j.jtemb.2016.05.001>
- [8] Gupta, S. K., Deshpande, R. D., Agarwal, M., & Raval, B. R. (2016). Origin of high fluoride in groundwater in the North Gujarat-Cambay region, India. *Hydrogeology Journal*, 24(3), 487-503. <https://doi.org/10.1007/s10040-015-1321-3>
- [9] Handa, B. K. (1975). Geochemistry and genesis of fluoride-containing ground waters in India. *Groundwater*, 13(3), 275-281. <https://doi.org/10.1111/j.1745-6584.1975.tb03086.x>
- [10] Jacks, G., Bhattacharya, P., Chaudhary, V., & Singh, K. P. (2005). Controls on the genesis of some high-fluoride groundwaters in India. *Applied Geochemistry*, 20(2), 221-228. <https://doi.org/10.1016/j.apgeochem.2004.07.002>
- [11] Jha, S. K., Nayak, A. K., & Sharma, Y. K. (2010). Fluoride occurrence and assessment of exposure dose of fluoride in shallow aquifers of Makur, Unnao district, Uttar Pradesh, India. *Environmental Monitoring and Assessment*, 167(1-4), 617-623. <https://doi.org/10.1007/s10661-009-1077-4>
- [12] Morales-Arredondo, J. I., Esteller, M. V., Martínez-Florentino, T. A. K., & Martínez-Morales, M. (2016). Fluorine concentrations in drinking water and its health effects in the volcanic region of Guadalajara, Mexico. *Environmental Geochemistry and Health*, 38(6), 1283-1295. <https://doi.org/10.1007/s10653-016-9799-7>
- [13] Mukherjee, I., & Singh, U. K. (2018). Groundwater fluoride contamination, probable release, and containment mechanisms: A review on Indian context. *Environmental Geochemistry and Health*, 40(6), 2259-2301. <https://doi.org/10.1007/s10653-018-0096-x>
- [14] Narsimha, A., & Sudarshan, V. (2017). Contamination of fluoride in groundwater and its effect on human health: A case study in hard rock aquifers of Siddipet, Telangana State, India. *Applied Water Science*, 7(5), 2501-2512. <https://doi.org/10.1007/s13201-016-0441-0>
- [15] Ozsvath, D. L. (2009). Fluoride and environmental health: A review. *Reviews in Environmental Science and Biotechnology*, 8(1), 59-79. <https://doi.org/10.1007/s11157-008-9136-9>
- [16] Reddy, A. G. S., Reddy, D. V., Rao, P. N., & Prasad, K. M. (2010). Hydrogeochemical characterization of fluoride rich groundwater of Wailpalli watershed, Nalgonda District, Andhra Pradesh, India. *Environmental Monitoring and Assessment*, 171(1-4), 561-577. <https://doi.org/10.1007/s10661-009-1298-6>
- [17] Reddy, D. V., Nagabhushanam, P., Sukhija, B. S., Reddy, A. G. S., & Smedley, P. L. (2020). Fluoride dynamics and monitoring in groundwater. In P. Bhattacharya, A. K. Mukherjee, K. Bundschuh, R. Zevenhoven, & R. H. Loeppert (Eds.), *Arsenic in the Environment: Biology and Chemistry* (Vol. 2, pp. 307-346). CRC Press.
- [18] Saxena, V. K., & Ahmed, S. (2003). Inferring the chemical parameters for the dissolution of fluoride in groundwater. *Environmental Geology*, 43(6), 731-736. <https://doi.org/10.1007/s00254-002-0672-2>
- [19] Sharma, D., Gupta, R., Singh, A., & Kanwar, R. (2017). Spatial and temporal distribution of fluoride in groundwater of Kota region, Rajasthan. *Journal of the*

- Geological Society of India*, 89(2), 165-170.
<https://doi.org/10.1007/s12594-017-0578-9>
- [20] Tekle-Haimanot, R., Melaku, Z., Kloos, H., Reimann, C., Fantaye, W., Zerihun, L., & Bjorvatn, K. (2006). The geographic distribution of fluoride in surface and groundwater in Ethiopia with an emphasis on the Rift Valley. *Science of the Total Environment*, 367(1), 182-190. <https://doi.org/10.1016/j.scitotenv.2005.11.003>
- [21] United States Environmental Protection Agency (USEPA). (2004). *Risk Assessment Guidance for Superfund Volume I: Human Health Evaluation Manual (Part E, Supplemental Guidance for Dermal Risk Assessment)*. Washington, DC: Office of Superfund Remediation and Technology Innovation.
- [22] United States Environmental Protection Agency (USEPA). (2017). *Regional Screening Levels (RSLs) - Generic Tables*. Retrieved from <https://www.epa.gov/risk/regional-screening-levels-rsls>
- [23] World Health Organization (WHO). (2017). *Guidelines for Drinking-Water Quality: Fourth Edition Incorporating the First Addendum*. Geneva: WHO Press.
- [24] Zhang, L., Zhao, L., Zeng, Q., Fu, G., Feng, B., Lin, X., Liu, X., & Hou, C. (2013). Spatial distribution of fluoride in drinking water and health risk assessment of children in typical fluorosis areas in North China. *Chemosphere*, 92(9), 1117-1122. <https://doi.org/10.1016/j.chemosphere.2013.01.081>